Biochimica et Biophysica Acta 1817 (2012) 370–380

Contents lists available at SciVerse ScienceDirect

Biochimica et Biophysica Acta

journal homepage: www.elsevier.com/locate/bbabio

Physiology and global gene expression of a *Corynebacterium glutamicum* ΔF_1F_O-ATP synthase mutant devoid of oxidative phosphorylation

Abigail Koch-Koerfges [a], Armin Kabus [a,1], Ines Ochrombel [b,2], Kay Marin [b,2], Michael Bott [a,*]

[a] Institut für Bio- und Geowissenschaften, IBG-1: Biotechnologie, Forschungszentrum Jülich, D-52425 Jülich, Germany
[b] Institut für Biochemie, Universität zu Köln, D-50674 Köln, Germany

ARTICLE INFO

Article history:
Received 29 August 2011
Received in revised form 14 October 2011
Accepted 18 October 2011
Available online 25 October 2011

Keywords:
F1FO-ATP synthase
Oxidative phosphorylation
atpBEFHAGDC deletion
Corynebacterium glutamicum
Proton motive force
Gene expression

ABSTRACT

A mutant of *Corynebacterium glutamicum* ATCC 13032 with a deletion of the *atpBEFHAGDC* genes encoding F_1F_O-ATP synthase was characterized. Whereas no growth was observed with acetate as sole carbon source, the ΔF_1F_O mutant reached 47% of the growth rate and 65% of the biomass of the wild type during shake-flask cultivation in glucose minimal medium. Initially, the mutant strain showed a strongly increased glucose uptake rate accompanied by a high oxygen consumption rate and pyruvate secretion into the medium. When oxygen became limiting, the glucose consumption rate was reduced below that of the wild type and pyruvate was consumed again. The ΔF_1F_O mutant had increased levels of *b*- and *d*-type cytochromes and a significantly increased proton motive force. Transcription of genes involved in central carbon metabolism was essentially unchanged, whereas genes for cytochrome *bd* oxidase, pyruvate:quinone oxidoreductase, oxidative stress response, and others showed increased mRNA levels. On the other hand, genes for amino acid biosynthesis and ribosomal proteins as well as many genes involved in transport displayed decreased mRNA levels. Several of the transcriptional changes were reflected at the protein level, but there were also discrepancies between the mRNA and protein levels suggesting some kind of posttranscriptional regulation. The results prove for the first time that F_1F_O-ATP synthase and oxidative phosphorylation are in general not essential for growth of *C. glutamicum*.

1. Introduction

Many aerobic respiring bacteria gain ATP both by substrate level phosphorylation (SLP) and by oxidative phosphorylation, or more generally electron transport phosphorylation (ETP). In this work, we addressed the question on the role of ATP synthesis by ETP using *Corynebacterium glutamicum*, a non-pathogenic, non-sporulating, facultatively anaerobic Gram-positive soil bacterium. This species has gained considerable interest for mainly two reasons. First, it is used for large scale biotechnological production of amino acids, predominantly L-glutamate (2.1 million tons/year) and L-lysine (1.1 million tons/year) [1]. Therefore, its metabolism is subject to intensive studies. Second, it serves as a model for the *Corynebacterineae*, a suborder of the *Actinomycetales* which includes a number of important pathogens, in particular *Mycobacterium tuberculosis*. An overview on *C. glutamicum* biology, genetics, physiology, and biotechnology can be found e. g. in recent monographs [1,2].

C. glutamicum possesses a respiratory type of energy metabolism and can use either oxygen or nitrate as terminal electron acceptors [3]. ATP can be synthesized either by SLP in glycolysis, in the tricarboxylic acid (TCA) cycle and by the conversion of acetyl-CoA to acetate or by ETP with the membrane-bound F_1F_O-ATP synthase using the proton motive force (pmf) as driving force. During aerobic growth of *C. glutamicum* pmf is mainly generated by the cytochrome bc_1-aa_3 supercomplex [4] with a postulated efficiency of 6 H^+/2 e^- and marginally by cytochrome *bd* oxidase [5] that translocates presumably 2 H^+/2 e^-. The measured H^+/O ratios [6] were in agreement with the proposed H^+/e^- ratios for the two branches of respiratory chain in *C. glutamicum* [3].

Although it is generally assumed that ETP is predominantly responsible for ATP synthesis in *C. glutamicum*, only few studies have addressed the role of F_1F_O-ATP synthase in this species. A mutant (strain F172-8) of *C. glutamicum* ATCC 14067 was described whose ATPase activity was decreased to 25% of the wild-type level due to a Ser273Pro point mutation in the γ subunit of F_1F_O-ATP synthase [7]. This mutant showed a pleiotropic phenotype. Glucose consumption per cell was increased by 70%, the respiration rate was doubled, large amounts of lactate as well as minor concentrations of pyruvate, L-alanine and L-valine were formed, whereas the formation of 2-oxoglutarate and proline was reduced compared to the parent strain. The ability to produce glutamate was almost completely lost. The phenotype of strain F172-8 was explained by the assumption that the defect in oxidative phosphorylation leads to a shortage of ATP, which in turn leads to an increased glucose catabolism. As a

* Corresponding author. Tel.: +49 2461 61 3294; fax: +49 2461 61 2710.
E-mail address: m.bott@fz-juelich.de (M. Bott).
[1] Present address: Momentive Performance Materials GmbH, D-51368 Leverkusen, Germany.
[2] Present address: Evonik Degussa GmbH, D-33790 Halle/Westfalen, Germany.

0005-2728/$ – see front matter © 2011 Published by Elsevier B.V.
doi:10.1016/j.bbabio.2011.10.006

consequence, the rate of NADH formation increases, leading to an increase of the respiration rate. The catabolism of pyruvate via the pyruvate dehydrogenase complex and the tricarboxylic acid cycle seems to be inhibited, leading to the absence of glutamate formation and via an increased pyruvate pool to the formation of lactate, alanine and valine [7]. Surprisingly, a later study reported that with stronger biotin limitation and lower inoculum size strain F172-8 showed higher glutamate production than the parent strain [8]. A proteome analysis of strain F172-8 published recently [9] will be described in the discussion section. As the mutant strain F172-8 still possessed 25% residual ATPase activity, the question whether F_1F_O-ATP synthase is essential for *C. glutamicum* remained open.

As in other bacteria the genetic order of the genes encoding the eight subunits of F_1F_O-ATP synthase (Fig. 1) in *C. glutamicum* is *atpBEFHAGDC* [7]. The promoter-proximal genes *atpB*, *atpE* and *atpF* encode the three components of the membrane-integral F_O part, i.e. the a, c and b subunit, respectively. The five subunits δ, α, γ, β and ε of the peripheral F_1-part are encoded by the promoter-distal genes *atpH*, *atpA*, *atpG*, *atpD* and *atpC*, respectively [7]. Studies on the transcriptional organization of the *atp* genes indicated that the *atpBEFHAGDC* cluster is transcribed as a 7.5 kb polycistronic mRNA from a promoter upstream of *atpB* [10]. The transcriptional start site of *atpB* was mapped 86 bp upstream of the predicted start codon of *atpB*, which leads to a protein of 322 amino acids. Evidence was obtained that the *atpBEFHAGDC* operon is induced at alkaline pH, possibly via the alternative sigma factor SigH [10].

In this study, we were able to create for the first time a defined mutant of *C. glutamicum* strain ATCC 13032 in which the entire *atpBEFHAGDC* operon was deleted. The properties of this ΔF_1F_O mutant were analyzed with respect to growth, by-product formation, cytochrome content, and bioenergetics. In addition, transcriptomics and proteomics were used to obtain a global view on the consequences at the level of gene expression. The results suggest that during growth on glucose the contribution of ETP to ATP synthesis in *C. glutamicum* is not as important as expected.

2. Materials and methods

2.1. Bacterial strains and culture conditions

C. glutamicum strains and plasmids used in this work are listed in Table 1. For analysis of growth, organic acid production, glucose and oxygen consumption, glycogen formation, measurement of internal pH, membrane potential ($\Delta\Psi$) and for RNA isolation, a 5 ml preculture in brain–heart infusion (BHI) medium supplemented with 2% (w/v) glucose was inoculated with colonies from a fresh agar plate (BHI agar + 2% (w/v) glucose) and incubated for 8 h at 30 °C and 170 rpm. Cells from the preculture were transferred to 20 ml CGXII minimal medium [11] containing 4% (w/v) glucose and cultivated for 16 h at 30 °C and 130 rpm. After washing the cells with 0.9% (w/v) NaCl the main culture with 50 ml CGXII minimal medium with 4% (w/v) glucose was inoculated to give an optical density at 600 nm (OD_{600}) of 1. The CGXII medium was always supplemented with 30 mg/l 3,4-dihydroxybenzoic acid as iron chelator. Main cultivations were done in baffled 500 ml Erlenmeyer flasks containing a septum for sterile sampling of the cultures with 50 ml medium at 30 °C and 130 rpm. Cells were harvested during the exponential growth phase at an OD_{600} of 4–6 for further analysis like DNA microarray experiments or pmf measurements. *Escherichia coli* DH5α, which was used as host for cloning, was cultivated in LB medium or on LB agar plates at 37 °C. When appropriate, kanamycin was used at a concentration of 25 μg/ml (*C. glutamicum*) or 50 μg/ml (*E. coli*).

2.2. DNA and RNA manipulations

Enzymes used for DNA restriction, ligation or dephosphorylation were obtained either from Roche Diagnostics (Mannheim, Germany) or New England Biolabs (Frankfurt am Main, Germany). Plasmid DNA from *E. coli* or *C. glutamicum* was isolated with the QIAprep Spin Miniprep kit according to the manufacturer's instructions (Qiagen, Hilden, Germany). Total RNA from *C. glutamicum* was isolated with the RNeasy kit according to the manufacturer's instructions (Qiagen).

2.3. Construction of an atpBEFHAGDC deletion mutant

An in-frame *atpBEFHAGDC* deletion mutant of *C. glutamicum* ATCC 13032 was constructed as described previously [12]. For this purpose, the *atpB* upstream region, including the first six codons of *atpB*, and the *atpC* downstream region, including the last seven codons of *atpC*, were amplified with the Expand High Fidelity kit (Roche Diagnostics) using the oligonucleotide pairs ΔF_1F_O-1-for/ΔF_1F_O-2-rev and ΔF_1F_O-3-for/ΔF_1F_O-4-rev, respectively (Table 2). The resulting PCR products of about 500 bp were subsequently fused by overlap-extension PCR to a product of approximately 1000 bp. After digestion with HindIII and XbaI, this fragment was cloned into pK19*mobsacB* [13], cut with the same restriction enzymes, to yield pK19*mobsacB*-ΔF_1F_O. DNA sequence analysis revealed that the cloned PCR product contained no unwanted mutations. Subsequently, plasmid pK19*mobsacB*-ΔF_1F_O was transferred by electroporation [14] into *C. glutamicum* strain ATCC 13032 and the transformation mixture was plated on a BHIS agar plate containing 25 μg kanamycin/ml. After selection for the first and second recombination event, kanamycin-sensitive and sucrose-resistant clones were analyzed by colony-PCR with the primer pair ΔF_1F_O-for/ΔF_1F_O-rev in order to distinguish between wild-type and ΔF_1F_O clones.

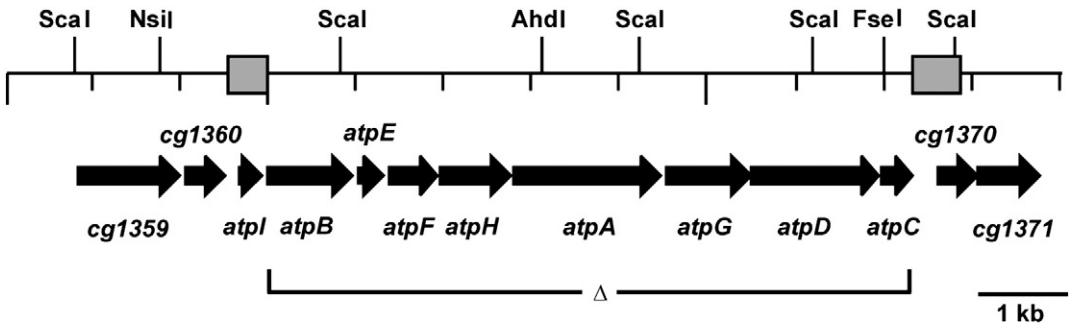

Fig. 1. Physical map of the *C. glutamicum atpIBEFHAGDC* gene cluster. cg1359, UDP-N-acetylglucosamine-1-phosphate transferase; cg1360, hypothetical membrane protein; *atpI*, hypothetical protein; *atpB*, a subunit of F_1F_0-ATP synthase; *atpE*, c subunit; *atpF*, b subunit; *atpH*, δ subunit; *atpA*, α subunit; *atpG*, γ subunit; *atpD*, β subunit; *atpC*, ε subunit; cg1370, hypothetical protein; cg1371, nuclease of the RecB family. The DNA region deleted in strain ΔF_1F_O is indicated. The gray bars indicate the regions amplified for construction of the plasmid pK19*mobsacB*-ΔF_1F_O.

Table 1
Strains and plasmids used in this study.

Strain or plasmid	Relevant characteristics	Source or reference
Strains		
C. glutamicum ATCC 13032	Wild type (wt), biotin auxotrophic	[56]
C. glutamicum ΔF_1F_O	ATCC 13032 derivative with a deletion of the *atpBEFHAGDC* genes	This work
E. coli DH5α	F^- Φ80*dlac*Δ(*lacZ*)M15 Δ(*lacZYA-argF*) U169 *endA1 recA1 hsdR17* (r_K^-, m_K^+) *deoR thi-1 phoA supE44*λ$^-$ *gyrA96 relA1*	Invitrogen (Karlsruhe, Germany)
Plasmids		
pK19*mobsacB*	Kan^R; vector for allelic exchange in *C. glutamicum* (pK18 $oriV_{E.c.}$, *sacB*, *lacZ*α)	[13]
pK19*mobsacB*-ΔF_1F_O	Kan^R, pK19*mobsacB* derivative containing a 1046 bp overlap-extension PCR product (HindIII/XbaI) which cover the flanking regions of the *C. glutamicum atpBEFHAGDC* genes	This work

2.4. Determination of growth parameters

Growth was followed by measuring optical density at 600 nm (OD_{600}) with an Ultrospec 500-pro spectrophotometer (Amersham Biotech). The biomass concentration was calculated from OD_{600} values using an experimentally determined correlation factor of 0.25 g CDW l^{-1} for $OD_{600} = 1$ [5].

2.5. Determination of glucose and organic acids

Quantitative determination of glucose and organic acids in culture supernatants was carried out by ion-exchange chromatography on a cation exchange column (Organic Acid Resin, CS chromatography, 300 × 8 mm) using isocratic elution within 40 min with 100 mM H_2SO_4 and a flow rate of 0.4 ml/min at 40 °C on an Agilent 1100 HPLC system (Agilent Technologies, Waldbronn, Germany). This newly developed method allows detection of organic acids by a diode array detector at 215 nm, and detection of glucose by a refraction index (RI) detector in the same run. The quantification of organic acids and sugar was based on a calibration curve with external standards. Additionally, the glucose concentration was determined with an enzymatic assay [15].

2.6. Determination of specific glucose uptake rates

Specific glucose uptake rates (sGUR) were calculated from glucose measurements and biomass concentrations using Eq. (1), where c_{glc} represents the glucose concentration (g l^{-1}), X_{CDW} the cell dry weight (CDW) per volume (g l^{-1}), and ($t_{i+1} - t_i$) the time interval (h) investigated:

$$sGUR(t_i, t_{i+1}) = \left(\frac{c_{glc,i} - c_{glc,i+1}}{t_{i+1} - t_i}\right) \cdot \left(\frac{2}{X_{CDW,i+1} + X_{CDW,i}}\right) \left[\frac{g_{glucose}}{g_{DW} \cdot h}\right]. \quad (1)$$

2.7. Determination of oxygen consumption

Oxygen consumption was determined as described [16] by following the decrease in dissolved oxygen (DO) using a shake flask reader (SFR) system (PreSens GmbH, Regensburg, Germany). The measurement is based on sensor spots containing a fluorophore with an O_2-dependent luminescent decay time. The sensor spot is illuminated by an optical fiber which also collects the emitted luminescent light. The luminescent decay time is related to the actual dissolved oxygen. For our experiments, the sensor spot was integrated into 500 ml baffled Erlenmeyer flasks containing a septum for fast sampling. The strains were cultivated in 50 ml CGXII minimal medium with 4% (w/v) glucose and incubated at 30 °C and 130 rpm. DO (% air saturation) was measured at an interval of 10 min.

2.8. Determination of the intracellular glycogen content

The cytoplasmic glycogen content of *C. glutamicum* was determined by an enzymatic method as described previously [17–19]. *C. glutamicum* cells from different growth phases (the volume of each sample depended on the amount needed to give 1 ml of a cell suspension with an OD_{600} of 50 for each time point) were harvested by centrifugation at 5000 × *g* and 4 °C for 5 min. Cells were washed twice in 2 ml of a cooled buffer containing 50 mM Tris–HCl and 50 mM NaCl (pH 6.3) and resuspended in 1 ml of 40 mM potassium acetate buffer (pH 4.2). This cell suspension corresponded to 12.5 mg CDW. After addition of 250 µl glass beads (Ø = 0.1 mm, Roth, Karlsruhe, Germany) and incubation for 5 min at 99 °C, cells were disrupted by 2 × 30 s bead-beating using a Silamat S5 (Ivoclar Vivadent GmbH, Ellwangen, Germany). Cell debris was removed by centrifugation (centrifuge 2K15, Sigma Laborzentrifugen, Osterode am Harz, Germany) at 13,000 rpm and room temperature for 20 min. 200 µl of the supernatant was transferred into two 1.5 ml reaction tubes (100 µl each) resulting in sample A (determination of glycogen) and sample B (determination of free glucose). After addition of 2 µl of an amyloglucosidase solution (10 mg/ml, Roche Diagnostics GmbH, Mannheim, Germany) to sample A, both samples were incubated at 100 rpm and 57 °C for 2 h. Subsequently, the glucose concentration in the two samples was determined via an enzymatic assay. The glucose concentration present as glycogen was calculated from the difference of sample A minus sample B. The glycogen amount per g CDW was determined according to Eq. (2), where c_{glc} represent the glucose concentration (mmol l^{-1}), M_{glc} the molar mass of glucose (180.16 mg $mmol^{-1}$), and 0.25 is the factor for converting OD_{600} to g CDW l^{-1}.

$$\text{Glycogen}\left[\frac{mg}{g_{CDW}}\right] = (c_{glc}(\text{sample A}) - (\text{sample B}))\left[\frac{mmol}{l}\right] \cdot \frac{M_{glc}}{OD_{600} \cdot 0.25}\left[\frac{mg \cdot l}{g_{CDW} \cdot mmol}\right] \quad (2)$$

2.9. Analysis of cytochromes

Dithionite-reduced spectra of intact cells resuspended in 0.9% (w/v) NaCl solution to an OD_{600} of 100 were recorded at room temperature

Table 2
Oligonucleotides used in this work. Restriction sites are underlined and complementary sequences of the primer pairs used for overlap-extension PCR are shown in italic.

Name	Sequence	Restriction enzyme
ΔF_1F_O-1-for	5′-TGACAAGCTTGAAACAGGGGAGTGGGG-3′	HindIII
ΔF_1F_O-2-rev	5′-*CCCATCCACTAAACTTAAACA*CAGGGGACGTGCTCCGCAA-3′	
ΔF_1F_O-3-for	5′-*TGTTTAAGTTTAGTGGATGGG*CGCAGCAGCGAAGGTCTCTAA-3′	
ΔF_1F_O-4-rev	5′-TCGACTCTAGACATAAAAACCGCCTCATC-3′	XbaI
ΔF_1F_O-for	5′-GACCTTCTACGACAACACCGCC-3′	
ΔF_1F_O-rev	5′-CTGGTGCTGCTTCCAACCAGGC-3′	

using 5 mm light path cuvettes with a Jasco V560 spectrophotometer equipped with a silicon photodiode detector for turbid samples [20]. For details see [12].

2.10. Determination of the proton motive force (pmf)

The pmf was determined as described previously [21]. Cells cultivated in CGXII minimal medium with 4% (w/v) glucose were harvested at an OD_{600} of 4–6 and the internal pH as well as the membrane potential ($\Delta\Psi$) was determined at external pH values of 7.0 and 6.0. For this purpose, the cells were washed three times in 250 mM MES buffer pH 6.0 containing 50 mM KCl or 250 mM MOPS buffer pH 7.0 containing 50 mM KCl. All washing and centrifugation steps were carried out on ice or at 4 °C. $\Delta\Psi$ was determined by measuring the distribution of [^{14}C]-tetraphenylphosphonium bromide (5 μM final concentration, specific radioactivity 0.995 Ci/mol) inside and outside the cells [22,23]. The pH gradient was determined by measuring the distribution of [^{14}C]-benzoic acid (15 μM final concentration, specific radioactivity 3.12 Ci/mol) inside and outside the cells. Corrections for unspecifically bound [^{14}C]-tetraphenylphosphonium bromide or [^{14}C]-benzoate were performed by using cells with collapsed membrane potential or pH gradient obtained by addition of the uncoupler carbonyl cyanide m-chloro phenyl hydrazone to a final concentration of 50 μM. Processing of samples for rapid separation of extra- and intracellular fluids was performed by using silicone oil centrifugation with perchloric acid in the bottom layer [23]. Corrections for the extracellular water space that cannot be removed by silicone oil centrifugation was performed by the addition of cell-impermeable [^{14}C]-labeled inulin and quantification of radioactivity in the bottom layer and the supernatant. The cell volume of *C. glutamicum* was determined by the determination of the distribution of freely permeable [^{3}H]-labeled H_2O (0.55 mCi/l) and [^{14}C]-labeled inulin (0.14 mCi/l) between the cell pellet and the supernatant [21]. All measurements were performed at least in triplicate and standard deviations were calculated.

2.11. Global gene expression analysis

DNA microarray analysis [24] was used to compare the genome-wide RNA concentrations of the ΔF_1F_O mutant and the *C. glutamicum* wild type. The strains were cultivated in CGXII minimal medium with 4% (w/v) glucose. RNA used for the synthesis of labeled cDNA was prepared from cells in the early exponential growth phase (OD_{600} ~5) and three independent DNA microarray experiments were performed, each starting from an independent culture. RNA isolation and synthesis of fluorescently labeled cDNA were carried out as described [25]. Custom-made DNA microarrays for *C. glutamicum* ATCC 13032 printed with 70mer oligonucleotides were obtained from Operon (Cologne, Germany) and are based on the genome sequence entry NC_006958 [26]. The arrays contained 3057 oligonucleotides for protein-coding genes, 1294 oligonucleotides for intergenic regions, 60 oligonucleotides for tRNA genes, 15 oligonucleotides for rRNA genes, and 140 oligonucleotides for positive and negative controls, plasmids and resistance genes. The experimental details for handling of these microarrays and for data evaluation were described previously [27].

2.12. Proteome analysis

Two-dimensional fluorescence difference gel electrophoresis (2-D DIGE) was performed using the Ettan™ DIGE System from GE Healthcare. Protein extracts were prepared from cells grown aerobically in CGXII minimal medium containing 4% (w/v) glucose at 30 °C and 130 rpm and harvested in the early exponential growth phase (OD_{600} ~5). Cell disruption, determination of protein concentration and protein precipitation was performed as described previously [28]. 200 μg of precipitated proteins were solubilized in 40 μl solubilization buffer (7 M urea, 2 M thiourea, 4% (w/v) CHAPS, 30 mM Tris–HCl, pH 8.5) by vigorous shaking for 1 h at room temperature. 100 μg of each sample were labeled independently with 400 pmol of a CyDye DIGE Fluor minimal dye (GE Healthcare, Cy3 for the wild type, Cy5 for the mutant, and Cy2 for the internal standard, which represents 100 μg of a mixture of equal amounts of all biological samples of the experiment) and incubated 30 min on ice in the dark. All subsequent steps were also carried out in the dark. To avoid deviation by labeling efficiency one color swop experiment was performed. The reaction was stopped by the addition of 10 mM lysine. The samples were filled up with 24 μl sample buffer (8 M urea, 130 mM DTT, 4% (w/v) CHAPS, 2% Pharmalyte 3–10) and were combined (Cy3-labeled wild type, Cy5-labeled ΔF_1F_O mutant, and Cy2-labeled internal standard). The mixture was filled up to a total volume of 450 μl with rehydration buffer (8 M urea, 13 mM DTT, 4% (w/v) CHAPS, 1% Pharmalyte 3–10) centrifuged at 17,608 × *g* at 4 °C for 5 min and the supernatant was used for isoelectric focusing (IEF). IEF was performed using Immobiline Dry-Strips (24 cm, pH 4–7 (linear); GE Healthcare) and an IPGphor electrophoresis unit. Electrophoresis parameters were: 50 μA/strip at 20 °C, rehydration 10 h, 500 V for 1 h, gradient to 1000 V for 4 h, gradient to 8000 V for 3 h, 8000 V for 5.36 h. Immobiline DryStrips were then equilibrated as recommended by the manufacturer and second-dimensional separation was performed using an Ettan™ DALT*six* electrophoresis unit (GE Healthcare) with 12.5% lab-cast SDS-polyacrylamide gels at 30 °C. After a 45 min forerun (200 V, 10 mA/gel and 2 W/gel) the main run was performed for 4.5 h (425 V, 40 mA/gel and 17 W/gel). The run was completed once the bromophenol blue marker reached the bottom of the gel. Afterwards the gels were scanned with a Typhoon Trio™ Variable Mode Imager (GE Healthcare) using either green, red or blue laser (532 nm, 633 nm, 488 nm) with corresponding emission filters (580, 670, 520) and a resolution of "200 μm" for the dyes Cy3, Cy5 and Cy2, respectively. The image analysis was performed using Delta2D 4.0 software (Decodon, Greifswald, Germany). Proteins were identified as significantly changed when the average of the ratio of deletion mutant to wild type was ≥1.5 or ≤0.6 and the p-value ≤0.05. Afterwards the gels were additionally stained with Coomassie brilliant blue and protein spots were cut from the gels using a Bio-Rad EXQuest Spot Cutter and gel plugs were placed into 96-well plates. Proteins were subjected manually to tryptic in-gel digestion [28] for subsequent identification by mass spectrometry. After tryptic digestion the peptide mixtures were transferred on Prespotted Anchor Chips (PAC) targets (Bruker Daltonics, Bremen, Germany) containing prespotted α-cyano-4-hydroxycinnamic acid as matrix. MALDI-TOF mass spectrometry was performed with an Ultraflex III TOF/TOF mass spectrometer (Bruker Daltonics). Mascot algorithm (Matrix Science, v.2.2.0) was used to compare the experimentally determined peptide mass patterns with those of the entire *C. glutamicum* proteome. Search parameters allowed for variable modifications due to methionine oxidation and one missed cleavage site. The molecular weight search (MOWSE) scoring scheme [29] was used for unequivocal identification of proteins and peptides.

3. Results

3.1. Growth and glucose consumption of a ΔF_1F_O mutant of C. glutamicum

In order to test the relevance of F_1F_O-ATP synthase for growth and physiology of *C. glutamicum*, a mutant lacking the *atpBEFHAGDC* genes (Fig. 1) coding for subunits a, b, c, α, β, γ, δ, and ε was constructed. The eight genes were replaced by a 21-bp sequence tag and only the six 5′-terminal codons of *atpB* and the seven 3′-terminal codons of *atpC* remained within the chromosome. The genomic structure of the mutant was verified by PCR with the oligonucleotide pair ΔF_1F_O-for/ΔF_1F_O-rev, which resulted in a PCR product of the expected size of 1.27 kb (data not shown). Initial growth tests on agar plates with CGXII minimal medium containing either 222 mM glucose or 100 mM

acetate as sole carbon source revealed that the mutant was able to grow with glucose, albeit much slower than the wild type, but not with acetate (Fig. S1). Acetate catabolism is initiated by the ATP-dependent phosphorylation to acetylphosphate by acetate kinase and subsequent conversion to acetyl-CoA by phosphotransacetylase [30]. In the tricarboxylic acid cycle, one ATP can be directly formed in the succinyl-CoA synthetase reaction [31]. Thus, no net ATP synthesis by SLP is possible during growth on acetate, explaining the inability of the ΔF_1F_O mutant to grow on acetate as sole carbon source. As shown in Fig. 2A, the ΔF_1F_O mutant was able to grow in CGXII minimal medium with 4% (w/v) glucose as sole carbon and energy source with 47% of the growth rate of the wild type ($0.19 \pm 0.02\ h^{-1}$ vs. $0.40 \pm 0.01\ h^{-1}$) and reached 65% of the biomass of the wild type ($10.3 \pm 0.5\ g(CDW)l^{-1}$ vs. $15.8 \pm 3\ g(CDW)l^{-1}$). These results prove for the first time that F_1F_O-ATP synthase is not essential for growth of *C. glutamicum*.

As shown in Fig. 2B, glucose was continuously taken up by the wild type and was completely consumed after 24 h. The maximal specific glucose uptake rate (sGUR) was $89 \pm 1\ nmol\ min^{-1}(mg\ CDW)^{-1}$ (Table 3, Fig. S2A). In contrast, glucose uptake by the ΔF_1F_O mutant exhibited biphasic kinetics with a change after 5–11 h and glucose consumption was finished after 30 h. Within the first hours of cultivation, the calculated sGUR reached values $\geq 328 \pm 72\ nmol\ min^{-1}(mg\ CDW)^{-1}$(Table 3, Fig. S2A), which are more than threefold higher than in the wild type. In the second phase, the sGUR values were in the range of $21 \pm 16\ nmol\ min^{-1}(mg\ CDW)^{-1}$ and thus much lower than in the wild type (Table 3).

3.2. Oxygen consumption, glycogen content and formation of organic acids by the ΔF_1F_O mutant

In order to find an explanation for the biphasic glucose uptake of the mutant, oxygen consumption was measured by optical sensing of the dissolved oxygen (DO) using an SFR system (see Materials and methods). As shown in Fig. 2C, oxygen consumption by the ΔF_1F_O mutant was initially much faster than by the wild type, whereas the growth rate of the mutant was lower, suggesting that the mutant has a significantly higher respiration rate. After about 7–8 h, the DO concentration in the mutant culture approached zero and oxygen became limiting. Thus, the decrease in the glucose uptake rate correlated with the beginning of oxygen limitation.

When growing in glucose minimal medium, *C. glutamicum* was recently shown to form significant amounts of glycogen in the beginning of the exponential growth phase, which are degraded at the late stages of the exponential growth phase [17]. To test whether the increased glucose uptake rate of the ΔF_1F_O mutant in the first phase of cultivation is accompanied by increased glycogen content, this parameter was determined in the mutant and the wild type throughout cultivation. As shown in Fig. 2E, the kinetics of changes in glycogen content in the wild type was similar to that reported before [17], but the absolute values were lower, with a maximum of $25.3 \pm 5.0\ mg\ glycogen\ (g\ CDW)^{-1}$. In the ΔF_1F_O mutant, the kinetics was similar as in the wild type, but the absolute values were reduced by about 50%, reaching a maximum of $11.2 \pm 4.1\ mg\ glycogen\ (g\ CDW)^{-1}$.

As an alternative to an increased glycogen accumulation, the metabolic imbalance in the ΔF_1F_O mutant could cause the excretion of higher amounts of organic acids. In fact, right from the start of the cultivation, the mutant secreted pyruvate into the medium (Fig. 2D), reaching a maximal specific concentration of $5.2 \pm 1.16\ mmol\ (g\ CDW)^{-1}$ after 8 h (4.0 mM in supernatant). No other organic acids were detected by HPLC in this period. After 8 h, upon the onset of oxygen limitation and the decrease in the glucose uptake rate, pyruvate was consumed again. In contrast to the ΔF_1F_O mutant, the wild type did not secrete pyruvate (Fig. 2D, Table 3). During oxygen limitation, both the ΔF_1F_O mutant and the wild type excreted mainly lactate with maximal concentrations of about 150 mM reached after 24 h by the wild type and after 32 h by the ΔF_1F_O mutant (Fig. 2G). Lactate accumulation was accompanied by a decrease of the pH and the subsequent lactate utilization by an increase of the pH (Fig. 2F). In addition to lactate, acetate (Fig. 2H), succinate (Fig. 2I), malate (Fig. 2J) and minor amounts of fumarate (Fig. S2B) were formed by the ΔF_1F_O mutant and the wild type. In all three cases, about 3-fold higher specific concentrations of these acids were formed by the mutant cultures (Table 3).

3.3. Alterations of the proton-motive force and respiratory chain composition in the ΔF_1F_O mutant

It is generally assumed that F_1F_O-ATP synthase is a major consumer of the proton-motive force (pmf) generated by respiration. The absence of this enzyme might influence the pmf and the composition of the respiratory chain. In order to calculate the pmf, the pH gradient (ΔpH) and the membrane potential ($\Delta\Psi$) of the mutant and the wild type were measured at external pH values of 7.0 and 6.0. At a neutral pH of 7.0 pmf is comprised nearly exclusively of $\Delta\Psi$. At an acidic external pH of 6.0 the pH gradient across the cytoplasmic membrane of more than one pH unit significantly contributes to the pmf [21]. As listed in Table 4, the internal pH was similar in ΔF_1F_O mutant and wild type at both external pH values, resulting in similar ΔpH values for the two strains. The $\Delta\Psi$ and pmf values determined for the wild type were in the range published previously for *C. glutamicum* [21]. However, $\Delta\Psi$ was significantly increased in the mutant cells corresponding to a considerable increase in the pmf of the ΔF_1F_O mutant by 15% at an external pH of 7.0 and by 21% at an external pH of 6.0 compared to the wild type. In order to determine the effect of a F_1F_O-ATP synthase deletion on the composition of the respiratory chain, dithionite-reduced spectra of cell suspensions of the ΔF_1F_O mutant and the wild type were recorded. The cells were harvested in the stationary growth phase after 24 h of cultivation. As shown in Fig. 3, the level of *b*- and *d*-type cytochromes was significantly increased in the ΔF_1F_O mutant. This result was in agreement with DNA microarray data, where the cytochrome *bd* oxidase encoding genes *cydA* and *cydB* showed 3.5-fold and 3.7-fold higher levels in the ΔF_1F_O mutant compared to the wild type (see below).

3.4. Comparative transcriptome analysis of ΔF_1F_O mutant and wild type

The characterization of the F_1F_O-ATP synthase deletion strain revealed significant differences in comparison to wild type cells, e.g. in growth, glucose consumption and the bioenergetic homeostasis. In order to address the reflection of these changes on a more global level, the transcriptomes of the ΔF_1F_O mutant and the wild type were compared by DNA microarray analysis. To investigate the effect of the F_1F_O-ATP synthase deletion on global gene expression, the transcriptomes of the ΔF_1F_O mutant and the wild type were compared by DNA microarray analysis. Both strains were cultivated in glucose minimal medium und RNA was isolated from cells in the exponential growth phase at an OD_{600} of about 5. The comparison was performed in triplicate starting from independent cultures. Overall, 131 and 159 genes showed a $\geq$2-fold increased or decreased mRNA level in the ΔF_1F_O mutant, respectively, with a p-value ≤ 0.05. The corresponding genes, their annotated functions, the mRNA ratios and the p-values are listed in Table S1. In Table 5, these genes were ordered into functional categories, which led to the following major observations: (i) Expression of the genes involved in glucose uptake, glycolysis, the pentose phosphate pathway, glycogen formation and degradation were not changed, although the glucose consumption rate of the ΔF_1F_O mutant was strongly increased in the initial phase of cultivation. Regarding the genes of the pyruvate dehydrogenase complex and the TCA cycle, a 2- to 2.5-fold increase of the mRNA level of *aceF*, *fum* and *mdh* was observed, whereas expression of the other genes remained unchanged. Genes involved in acetate and ethanol catabolism (*ackA*, *pta*, *adhA*, *ald*)

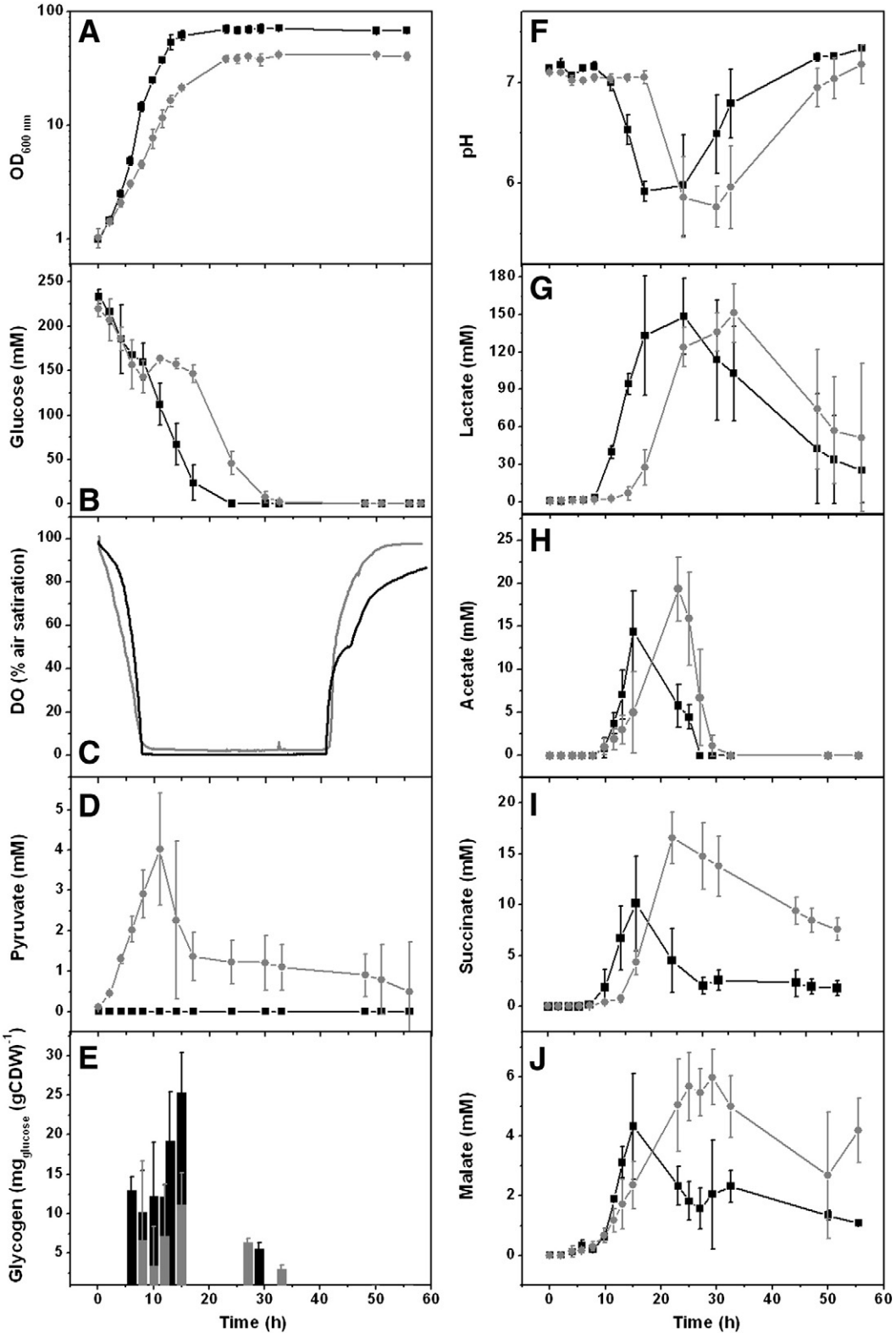

Fig. 2. Comparison of *C. glutamicum* wild type and its ΔF_1F_O mutant with respect to growth (A), glucose consumption (B), dissolved oxygen (C), pyruvate formation (D), glycogen formation (E), pH of the supernatant (F), lactate formation (G), acetate formation (H), succinate formation (I), and malate formation (J). The strains were cultivated in CGXII medium with 4% (w/v) glucose using shake flasks. The wild type is indicated by black symbols, curves, or bars, the ΔF_1F_O mutant by gray symbols, curves or bars. Mean values and standard deviation from of at least three independent cultivations of each strain are shown except for the DO measurements (panel C), where a representative experiment from three independent measurements is shown.

and the glyoxylate shunt (*aceA*, *aceB*) were slightly down regulated in the mutant. (ii) With respect to respiration and oxidative phosphorylation, a 2.5-fold increased expression of the *pqo* gene for pyruvate:menaquinone oxidoreductase was observed in the ΔF_1F_O mutant, whereas *lldD* gene for the quinone-dependent L-lactate dehydrogenase showed a 4-fold reduced mRNA level. Expression of all other known or proposed

Table 3
Growth parameters, specific glucose uptake rate (sGUR), pH values and organic acid formation by *C. glutamicum* wild type and the ΔF_1F_O mutant during cultivation in CGXII minimal medium with 4% (w/v) glucose. Mean values from at least three independent experiments and standard deviations (σ) are given. The values given for glycogen, pyruvate, lactate, acetate, succinate, malate and fumarate represent the maxima observed during growth.

Parameter	ATCC 13032	σ	ATCC 13032ΔF_1F_O	σ
OD_{600}	63	±12	41	±2
Cell dry weight (CDW) (g l^{-1})	15.8	±3	10.3	±0.5
μ (h^{-1})	0.40	±0.01	0.19	±0.02
sGUR (nmol min^{-1} (mg CDW)$^{-1}$)				
Within the 1st 11 h	89	±0.6	328	±72
Within 14–24 h			21	±16
Glycogen content$_{max}$ (mg (g CDW)$^{-1}$)	25.3	±5.0	11.2	±4.1
pH_{max}	7.5	±0.1	7.8	±0.1
pH_{min}	5.9	±0.1	5.8	±0.2
Pyruvate$_{max}$ (mM)	0	–	4.02	±1.38
Pyruvate$_{max}$ (mmol (g CDW)$^{-1}$)	0	–	5.20	±1.16
Lactate$_{max}$ (mM)	149	±31	151	±42
Lactate$_{max}$ (mmol (g CDW)$^{-1}$)	13.0	±5.0	17.5	±4.3
Acetate$_{max}$ (mM)	14.4	±4.7	19.3	±3.7
Acetate$_{max}$ (mmol (g CDW)$^{-1}$)	0.74	±0.50	2.16	±0.67
Succinate$_{max}$ (mM)	10.1	±4.7	16.6	±2.6
Succinate$_{max}$ (mmol (g CDW)$^{-1}$)	0.74	±0.27	2.07	±0.76
Malate$_{max}$ (mM)	4.3	±1.7	6.0	±0.94
Malate$_{max}$ (mmol (g CDW)$^{-1}$)	0.27	±0.14	0.68	±0.06
Fumarate$_{max}$ (mM)	0.06	±0.01	0.77	±0.24
Fumarate$_{max}$ (mmol (g CDW)$^{-1}$)	0.01	±0.01	0.09	±0.03

dehydrogenase genes (*ndh*, *mqo*, *sdhCAB*, *dld*, *glpD*, *putA*) was comparable to the wild type situation. The *cydAB* genes encoding the terminal cytochrome *bd* oxidase were up-regulated by a factor of 3.5 in the ΔF_1F_O mutant, whereas expression of the cytochrome bc_1-aa_3 supercomplex genes (*qcrCAB*, *ctaCDEF*) was similar in both strains. (iii) 13 genes involved in different amino acid biosynthesis pathways and 20 genes encoding ribosomal proteins showed a decreased mRNA level in the ΔF_1F_O mutant, indicating a reduced protein synthesis capacity. In addition, the *rpoA* gene encoding the α-subunit of RNA polymerase was expressed at a two-fold reduced level. (iv) Genes involved in sulfate reduction to sulfide and in sulfonate utilization displayed 2- to 4-fold increased mRNA levels in the ΔF_1F_O mutant. (v) Many genes involved in the response to oxidative stress showed a 2- to 4.5-fold increased expression in the ΔF_1F_O mutant. These included the ones encoding catalase (*katA*), superoxide dismutase (*sodA*), ferritin (*ftn*), the starvation-induced DNA protecting protein (*dps*), the Suf iron-sulfur cluster assembly and repair machinery (cg1764–cg1759), a putative multi-copper oxidase (cg1080), the transcriptional regulators SufR, OxyR, DtxR, WhcA [32,33] and WhcE [34]. Further stress genes showing an increased expression in the ΔF_1F_O mutant were those encoding a universal stress protein (*uspA1*), an ATPase subunit of the Clp protease (*clpX*), a putative protease modulator (*ppmA*; [25]), and the alternative sigma factor SigE [35]. Moreover, several additional transcriptional regulators showing an altered expression are presumably involved in stress responses. (vi) 15 genes encoding proteins involved in the transport of metabolites, ions or proteins showed an increased expression, whereas 49 genes of this category showed a decreased expression in the mutant.

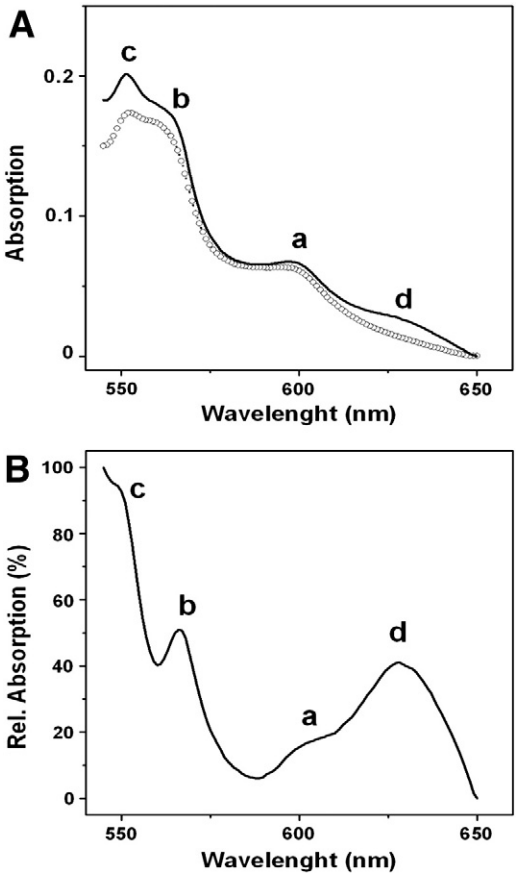

Fig. 3. A, dithionite-reduced spectra of intact cells from the stationary phase of the wild type (-○-) and the ΔF_1F_O mutant (—). The characteristic absorption maxima of the *a*-, *b*, *c*- und *d*-type cytochromes (600 nm, 562 nm, 552 nm, and 630 nm, respectively) are indicated. B, difference spectrum (ΔF_1F_O minus wild type) calculated from standardized absolute spectra.

3.5. Comparative proteome analysis of ΔF_1F_O and wild type

In addition to the transcriptome studies, a comparison of a fraction of the soluble proteome was performed. For this purpose cells were harvested in early exponential growth phase (OD_{600} 5–6) and cytoplasmic proteins were analyzed by two-dimensional fluorescence difference gel electrophoresis (2-D DIGE) in the pH range 4–7. Using Delta2D 4.0 software for data analysis, a comparison of the dye-labeled proteomes allowed the identification of 25 protein spots with an increased level and of 32 protein spots with a decreased level in the deletion mutant. After tryptic digestion and peptide mass fingerprinting using MALDI-TOF-MS, 21 proteins with a ≥1.5-fold increased level and 18 proteins with a ≤0.6-fold decreased level were identified. In Table 6, the protein ratios and, for comparison, the mRNA ratios of the corresponding genes are listed and compared to the protein ratios reported for exponentially growing cells of strain F172-8 vs. it parent strain [9]. The following observations were made: (i) several enzymes involved in central carbon metabolism showed

Table 4
Bioenergetic parameters (pH gradient ΔpH, membrane potential ΔΨ, and proton motive force pmf) determined for *C. glutamicum* wild type and the ΔF_1F_O mutant. Mean values from at least three independent experiments and standard deviations (σ) are given.

Strain	pH_{ex}	pH_{in}	σ	ΔpH	σ	ΔpH (mV)	σ	ΔΨ (mV)	σ	pmf (mV)	σ
ATCC 13032	7	7.51	0.07	0.50	0.05	−30	3	−192	2	−222	3
ATCC 13032ΔF_1F_O	7	7.59	0.04	0.59	0.04	−35	2	−220	<1	−255	3
ATCC 13032	6	7.09	0.04	1.09	0.04	−65	3	−131	7	−196	9
ATCC 13032ΔF_1F_O	6	7.11	0.20	1.11	0.20	−67	11	−172	3	−239	12

Table 5
Functional categories of genes showing an at least 2-fold altered mRNA level in the ΔF_1F_O mutant compared to the wild type. Genes whose mRNA ratio is ≥4 or ≤0.25 are shown in boldface, those with an mRNA ratio ≥10 or ≤0.25 are indicated in boldface and shaded in gray.

Functional category	mRNA ratio ΔF_1F_O/wild type					
	≥10.0	**≥4.0**	≥2.0	≤0.50	**≤0.25**	**≤0.10**
Pyruvate dehydrogenase complex and TCA cycle	*aceF*, *mdh*, *fum*					
Acetate and ethanol metabolism, glyoxylate shunt				*ackA*, *pta*, ***adhA***, ***ald***, *aceA*		
Respiration and oxidative phosphorylation	*cydA*, *cydB*, *cydD*, *pqo*			***atpB***[1], ***atpE***[1], ***atpF***[1], ***atpH***[1], ***atpA***[1], ***atpG***[1], ***atpD***[1], ***atpC***[1], ***lldD***		
Anaplerosis and gluconeogenesis	*pck*			***pyc***, *malE*		
Nitrogen assimilation	*gdh*, *glnA2*					
Amino acid biosynthesis	*dapD*			*leuA*, *ilvB*, ***argJ***, ***argB***, ***argD***, ***argF***, *metX*, ***metE***, *aroF*, ***aroE3***, *trpP*, *trpG*, *trpD*		
Sulfate reduction and sulfonate utilization	*cysK*, *cysN*, *cysD*, ***cysH***, *cysI*, ***cysJ***, *ssuR*, *ssuI*, *ssuD2*, *ssuC*					
Other metabolic enzymes	**cg0238**, *dtsR1*, *galE*, cg1405, *ispG*, *treZ*, *treS*, *butA*, cg3323			*iolD*, *iolE*, *iolG*, *iolH*, *emb*, *rmlB2*, ***prpD2***, ***prpB2***, ***prpC2***, *fas-IB*, cg1458, *carA*, *pyrC*, *nagD*, *vanB*, *catA1*, *gntK*, *cps*		
Biosynthesis of cofactors and prosthetic groups	cg0898, cg0899, cg1203, *nadA*, ***thiC***, *thiE*, ***hemH***, *ctaA*			*panB*, ***panC***		
RNA and DNA synthesis	*uvrB*			*rpoA*, *dnaQ*, *cglIIR*, *ssb*		
Translation				*rplJ*, *rpsJ*, *rplD*, *rplW*,*rplB*, *rpsS*, *rplV*, *rpsC*, *rplP*, *rpsH*, *rplF*, *rplR*, *rpsE*, *rpmD*, *infA*, *rpsK*, *rpsD*, *rplQ*, *groEL′*, *prsP-1*, *rpsO*, *rpsF*		
Response to oxidative and other stresses	***katA***, *whcA*, *whcE*, cg1080, **cg1759**, ***sufU***, ***sufS***, *sufC*, ***sufD***, ***sufB***, ***sufR***, *ftn*, *sodA*, *dps*, *oxyR*, *dtxR*, *sigE*, ***ppmA***, *clpX*, *uspA1*			*uspA2*, *rosR*		
Transcriptional regulators	*cgtS10*, *cgtR10*, *sigE*[2], ***sufR***[2], *dtxR*[2], *oxyR*[2], *whcA*[2], *whcE*[2], *phoR*, cg2889			cg0537, *rosR*[2], cg1392, cg3202, cg3303		
Transport of metabolites, inorganic ions and proteins	**cg1081**, cg1101, *czcD*, *secA2*, *tatA*, *pacL*, *terC*, cg2675, cg2676, cg2677, cg2678, cg2810, **cg3112**, cg3399			***ptsS***, cg0045, cg0082, cg0087, **cg0133**, *mnhF*, *mnhE*, *mnhD*, *mnhC*, **cg0506**, **cg0507**, **cg0508**, *pitA*, cg0622, **cg0623**, cg0735, cg0831, cg0832, *msiK2*, ***mctC***, *porB*, cg1289, cg1834, cg1836, *gluA*, *gluB*, *gluC*, **cg2181**, cg2182, **cg2183**, cg2184, cg2468, **cg2470**, *ectP*, **cg2550**, cg2551, cg2610, *vanK*, cg2704, *amyE*, *pstB*, *pstA*, ***pstC***, ***pstS***, cg2911, *gntP*, **cg3226**, *proP*, cg3404		
Genes with a predicted function	cg0237, cg0358, cg0387, cg0662, cg0686, cg0998, cg1068, cg1073, cg1080, cg1127, **cg1292**, cg1423, cg1628, cg1740, cg1745, cg1881, cg2417, cg2589, cg2612, **cg2796**, cg2890, cg2962, **cg3140**			cg0134, **cg0624**, cg0961, cg1578, cg1837, *tnp2f* (IS*Cg2*f), cg2166, cg2732, **cg3195**, cg3374		
Genes of unknown function	**cg0018**, cg0195, cg0241, cg0316, cg0706, cg0923, cg1082, **cg1091**, cg1092, cg1106, cg1158, cg1202, cg1286, cg1293, cg1408, cg1475, cg1514, **cg1626**, cg1742, **cg1746**, cg1822, cg1823, cg1931, cg2350, **cg2564**, cg2699, cg2797, cg2799, cg2850, cg3113, cg3117, cg3263			cg0286, cg0322, cg0323, cg0325, cg0607, cg0621, **cg0625**, cg0715, **cg0896**, cg0952, cg0958, cg1313, cg1614, cg1845, cg1908, cg1918, cg2080, cg2381, cg2389, cg2707, cg2828, cg3019, cg3189, cg3190, cg3260		

[1]The decreased mRNA ratio of the *atpBEFHAGDC* genes is caused by the deletion of these genes in the ΔF_1F_O mutant and thus serves as a control for the functionality of the DNA microarray analysis.
[2]These genes are also listed in the category "Response to oxidative and other stresses".

increased protein levels. Interestingly, the corresponding mRNA levels were unchanged in many cases (*pgm*, *pfkB*, *gpmA*, *gapA*, *icd*). This might be a hint for some kind of posttranscriptional regulation. (ii) Clearly increased levels were observed in the ΔF_1F_O mutant for proteins involved in the oxidative stress response, such as catalase, SufB, SufD, SufS and superoxide dismutase. For all these proteins, also the mRNA levels were increased. (iii) Several ribosomal proteins, elongation factors EF-2 and Ts as well as the chaperones DnaK, DnaJ2, GroEL, and GrpE showed decreased protein levels in the ΔF_1F_O mutant. In some cases, the mRNA levels were changed similarly, but in others the mRNA levels were unchanged (*fusA*, *tsf*, *dnaJ2*, *dnaK*, *grpE*), again suggesting posttranscriptional regulation. There are several reasons responsible for the much lower number of differences observed in the proteome comparison compared to the transcriptome comparison. For example, only a fraction of the entire proteome was analyzed by the 2D gels, the sensitivity of proteome analysis is lower than that of the DNA microarray analysis, and mRNA translation is subject to various regulatory mechanisms.

4. Discussion

In the present work, we investigated a mutant of *C. glutamicum* lacking ATP synthesis via oxidative phosphorylation due to a deletion of the *atpBEFHAGDC* genes. The fact that such a mutant could be isolated and was able to grow on substrates like glucose allowing SLP proves that F_1F_O-ATP synthase is not essential in general for this organism. Glucose catabolism by the ΔF_1F_O mutant showed two distinct phases, differentiated by the availability of the terminal electron acceptor oxygen. Under conditions of sufficient oxygen supply, glucose was consumed very rapidly, with calculated rates exceeding those of the wild type about 3-fold. This indicates that the flux capacity for glucose uptake and catabolism to pyruvate (via glycolysis or the pentose phosphate pathway) is only partially used by the wild type. The first limiting step appears to be the pyruvate dehydrogenase reaction, causing accumulation and export of pyruvate. The fact that pyruvate but not lactate was secreted by the mutant under conditions of oxygen excess supports the view that no limitation of NADH-reoxidation occurs in the ΔF_1F_O mutant under these conditions. Under oxygen limitation both the wild type and the mutant excreted high amounts of lactate, which is due to a limitation in NADH reoxidation. Also in *E. coli* higher glycolytic flux stimulated the secretion of pyruvate [36].

In contrast to the increased carbon flux, transcription of genes encoding components of the PTS uptake system and enzymes involved in glycolysis was not increased in ΔF_1F_O mutant or less than a factor of two. At the protein level, 1.5- to 2-fold increased levels of fructose bisphosphate aldolase, glyceraldehyde 3-phosphate dehydrogenase and phosphoglyceromutase were observed. The results suggest that control of the carbon flux from glucose to pyruvate occurs predominantly at the posttranscriptional level. In contrast to many other organisms, 6-phosphofructokinase of *C. glutamicum* is not influenced by AMP or ATP [37]. Currently, the most important control point for the glycolytic flux is considered to be pyruvate kinase [38], whose enzymatic activity is inhibited by ATP and activated by AMP [39,40]. However, as phosphoenolpyruvate is also converted to pyruvate by the phosphotransferase system, additional control points appear likely. In line with the enhanced rate of NADH formation in glycolysis, also the respiration rate of the ΔF_1F_O mutant was significantly increased (Fig. 2). The higher levels of *b*- and *d*-type cytochromes and the increased expression levels of the *cydA* and *cydB* genes encoding the two subunits of the cytochrome *bd* terminal oxidase indicate that this enzyme contributes to the increased respiration rate of the mutant.

When oxygen became limiting, glucose catabolism of the ΔF_1F_O mutant changed significantly. The glucose consumption rate decreased to values much lower than that of the wild type and large concentrations of lactate and in addition acetate, succinate and malate were formed.

Table 6
Proteins with a ≥2-fold altered amount in the ΔF_1F_O mutant as determined by 2-D DIGE analysis. For comparison the mRNA ratios of the corresponding genes are listed (n.c., no change). Proteins are ordered in functional categories. The protein ratio is the mean value from three independent experiments. For comparison, the protein ratios reported by Li and coworkers [9] for the F127-8 mutant vs. its parent strain are listed. SU, subunit.

Functional category		Protein ratio		mRNA ratio		Protein ratio
Locus tag	Protein	ΔF_1F_O/wild type	p-value	Gene	ΔF_1F_O/wild type	F127-8/wild type [9]
Glycolysis						
cg2800	Phosphoglucomutase	5.31	0.03	*pgm*	n.c.	
cg2119	1-Phosphofructokinase	3.56	<0.01	*pfkB*	n.c.	
cg0482	Phosphoglyceromutase	2.14	<0.01	*gpmA*	n.c.	1.62
cg3068	Fructose 1,6-bisphosphate aldolase	2.09	0.01	*fda*	1.78	1.55
cg1791	Glyceraldehyde 3-phosphate dehydrogenase	1.53	<0.01	*gapA*	n.c.	1.05
cg2291	Pyruvate kinase	n.c.		*pyc*	n.c.	2.38
cg1409	6-Phosphofructokinase	n.c.		*pfkA*	1.60	2.22
cg1790	3-Phosphoglycerate kinase	n.c.		*pgk*	n.c.	1.20
cg1789	Triosephosphate isomerase	n.c.		*tpi*	1.60	1.13
cg1111	Enolase	n.c.		*eno*	n.c.	1.02
TCA cycle, methylcitrate cycle, and glyoxylate shunt						
cg0949	Citrate synthase	3.09	<0.01	*gltA*	1.30	
cg0766	Isocitrate dehydrogenase	2.60	0.03	*icd*	n.c.	
cg2613	Malate dehydrogenase	2.25	<0.01	*mdh*	2.49	2.50
cg1737	Aconitase	1.79	0.02	*acn*	1.35	
cg2560	Isocitrate lyase	0.49	0.05	*aceA*	0.44	
cg0759	2-Methylcitrate dehydratase	0.29	<0.01	*prpD2*	0.16	
cg2192	Malate:quinone oxidoreductase	n.c.		*mqo*	1.80	4.30
cg3047	Acetate kinase	n.c.		*ackA*	0.30	2.39
cg1145	Fumarase	n.c.		*fum*	2.40	1.72
cg0447	Succinate dehydrogenase SU B	n.c.		*sdhB*	n.c.	1.38
Respiration and oxidative phosphorylation						
cg2891	Pyruvate quinone oxidoreductase	3.74	<0.01	*pqo*	2.50	1.64
cg1368	F_1F_O-ATP synthase β SU	Δ		*atpD*	0.06	2.19
cg1366	F_1F_O-ATP synthase α SU	Δ		*atpA*	0.03	1.75
cg1365	F_1F_O-ATP synthase δ SU	Δ		*atpH*	0.01	1.72
Response to oxidative stress						
cg0310	Catalase	2.72	<0.01	*katA*	4.39	2.39
cg1761	SufS, Fe-S cluster assembly protein	2.22	<0.01	*sufS*	4.32	
cg1763	SufD, Fe-S cluster assembly protein	2.20	0.02	*sufD*	3.98	
cg1764	SufB, Fe-S cluster assembly protein	1.93	0.01	*sufB*	4.09	
cg3237	Superoxide dismutase	1.47	<0.01	*sod*	3.18	
Translation and protein folding						
cg2499	Glycyl-tRNA synthetase	2.36	<0.01	*glyS*	1.66	
cg0587	Elongation factor Tu	1.99	<0.01	*tuf*	n.c.	
cg1072	50S Ribosomal protein L25	0.57	0.06	*rplY*	0.52	
cg0583	Elongation factor EF-2	0.47	0.05	*fusA*	n.c.	
cg2221	Elongation factor Ts	0.46	<0.01	*tsf*	n.c.	
cg2515	Molecular chaperone DnaJ2	0.46	<0.01	*dnaJ2*	n.c.	
cg0581	30S Ribosomal protein S12	0.45	0.04	*rpsL*	0.83	
cg2185	Prolyl-tRNA synthetase	0.39	<0.01	*proS*	0.81	
cg3011	Chaperonin GroEL	0.21	<0.01	*groEL*	0.55	
cg3100	Molecular chaperone DnaK	0.20	<0.01	*dnaK*	n.c.	
cg0572	50S Ribosomal protein L10	0.16	0.03	*rplJ*	0.49	
cg1531	30S Ribosomal protein S1	0.11	<0.01	*rpsA*	0.76	
cg3099	Molecular chaperone GrpE	0.07	<0.01	*grpE*	n.c.	
cg0573	50S Ribosomal protein L7/L12	0.03	<0.01	*rplL*	0.72	
Amino acid biosynthesis						
cg1432	Dihydroxy acid dehydratase	2.28	0.01	*ilvD*	n.c.	
cg1133	Serine hydroxymethyltransferase	1.97	0.01	*glyA*	1.22	
cg1487	Isopropylmalate isomerase, large subunit	0.39	<0.01	*leuC*	0.43	
Other metabolic enzymes						
cg0700	Inositol-5-monophosphate dehydrogenase	2.08	<0.01	*guaB3*	0.72	
cg1075	Ribose-phosphate pyrophosphokinase	0.33	<0.01	*prsA*	0.71	
Transporters						
cg2708	ABC-type sugar transport system, ATPase component	0.41	<0.01	*msiK1*	0.54	
Proteins of unknown function						
cg1091	Hypothetical protein	1.99	0.02		10.80	
cg2132	Hypothetical protein	0.28	0.01		0.75	

The same by-products were also formed by the wild type, but at lower levels (Table 3). As mentioned above, lactate formation by the NADH-dependent lactate dehydrogenase serves to reoxidize NADH. Acetate can be formed either from acetyl-CoA by phosphotransacetylase (*pta*) and acetate kinase (*ackA*), thereby generating ATP, or from pyruvate by pyruvate:quinone oxidoreductase. The latter enzyme converts pyruvate to acetate and CO_2 and uses menaquinone as electron acceptor [41]. Whereas the mRNA levels of *pta* and *ackA* were unchanged, that of *pqo* was increased about 2.5-fold in the ΔF_1F_O mutant and also the protein level was found to be 3-fold increased (Tables 5 and 6). This suggests that pyruvate:quinone oxidoreductase is relevant for pyruvate catabolism by the ΔF_1F_O mutant under oxygen limitation. Succinate and malate are intermediates of the TCA cycle. They can be formed either in the oxidative direction of the pathway or in the reductive direction, where oxaloacetate is reduced via malate and fumarate to succinate. This route was shown to operate under oxygen limitation [42] and

allows reoxidation of NADH and menaquinol by malate dehydrogenase (*mdh*) and succinate dehydrogenase (*sdhCAB*), respectively. The genes encoding malate dehydrogenase (*mdh*) and fumarase (*fum*) showed increased expression in the ΔF_1F_O mutant, suggesting that the reductive direction might be the favored one. Whereas the kinetics of glucose uptake by the ΔF_1F_O mutant was biphasic, the kinetics of growth was not (Fig. 2). Perhaps the formation of additional ATP by conversion of acetyl-CoA to acetate, which occurred only in the phase of lowered glucose consumption, might have compensated the decreased rate of ATP synthesis in glycolysis.

The transcriptome comparison of the ΔF_1F_O mutant and the wild type revealed a variety of gene expression changes. Many genes for amino acid biosynthesis and ribosomal proteins and also the *rpoA* gene for the α-subunit of RNA polymerase showed decreased expression, which presumably reflects the decreased growth rate of the mutant. On the other hand, many genes involved in the response to oxidative stress were found to have increased mRNA levels in the ΔF_1F_O mutant, including genes for destruction of reactive oxygen species (catalase, superoxide dismutase), genes for iron storage protein (ferritin, Dps), genes for the assembly and repair of iron sulfur clusters (Suf protein), and regulatory genes known or presumed to be involved in this response, such as *oxyR*, *sufR*, *whcA*, *whcE*, or *dtxR* (Table 5). Control of iron homeostasis by DtxR [43,44] is particularly important, as ferrous iron triggers the formation of reactive oxygen species *via* the Fenton reaction [45]. In accordance with the transcriptome data, the proteome comparison revealed increased levels of catalase, superoxide dismutase, and several Suf proteins (Table 6). The triggering of the oxidative stress response is most likely due to the increased respiration rate of the mutant, which causes an increased formation rate of reactive oxygen species, e.g. by the cytochrome bc_1 complex [46].

A proteome comparison of strain *C. glutamicum* F172-8 and its parent revealed moderately increased protein levels of some glycolytic enzymes (in particular 6-phosphofructokinase and pyruvate kinase), of some enzymes of the TCA cycle (in particular malate:quinone oxidoreductase and malate/lactate dehydrogenase MdhB), of some subunits of the F_1F_O-ATP synthase and of pyruvate:quinone oxidoreductase, acetate kinase and catalase (Table 6, [9]). Some of these changes are in accord with our findings, whereas others are not, which might be due to the different host strains used and to the fact that the F172-8 mutant in contrast to the ΔF_1F_O mutant still possesses 25% residual ATPase activity.

The observation that F_1F_O-ATP synthase is not essential for growth on substrates allowing SLP was previously also made for ΔF_1F_O mutants of *E. coli* [47,48] and *Bacillus subtilis* [49]. On the other hand, F_1F_O-ATP synthase was reported to be essential for *M. tuberculosis* [50,51] and *Mycobacterium smegmatis* [52], which are close phylogenetic relatives of *C. glutamicum*. The reason for this difference is not known yet. In Table 7, a comparison of different parameters determined for the ΔF_1F_O mutants of *C. glutamicum*, *E. coli* and *B. subtilis* is shown. With respect to the growth rate, the decrease in the case of *C. glutamicum* was stronger than for *B. subtilis* and in particular *E. coli*, whereas the growth yield was reduced somewhat less for *C. glutamicum* than for *E. coli* and *B. subtilis*. The respiration rate was increased for all three mutants, the membrane potential was increased in *C. glutamicum* and *E. coli* (not determined for *B. subtilis*), the ATP/ADP ratio was decreased in *E. coli* and *B. subtilis* (not determined for *C. glutamicum*) and cytochromes of the *b*- and *d*-type were increased in *C. glutamicum* and *E. coli* (not determined for *B. subtilis*). In the case of *B. subtilis*, increased expression of the genes encoding subunit I of cytochrome caa_3 oxidase and of subunit II of the cytochrome aa_3 quinol oxidase was observed [49]. Thus, despite the fact that the ΔF_1F_O mutants were derived from species of three different phyla (Proteobacteria, Firmicutes, Actinobacteria), they show many similar properties, indicating that the control of carbon flux by the energy status of the cell is evolutionary conserved [53]. Moreover, the results suggest that the proportion of ATP gained by oxidative phosphorylation is probably not as large as assumed by theoretical calculations in which the P/O ratio is determined under the assumption that the proton motive force (pmf) is used exclusively by F_1F_O-ATP synthase for ATP synthesis. Assuming that 1 mol ATP allows the synthesis of 10 g cell dry weight [54,55], the *C. glutamicum* ΔF_1F_O mutant formed 4.55 mol ATP/mol glucose consumed, a value that fits roughly with the expectation for the ATP yield from glucose by SLP only. Under the assumption that also the wild type requires 1 mol ATP for 10 g cell dry weight, it formed 7.2 mol ATP/mol glucose, corresponding to an increase of only 58% compared to the ΔF_1F_O mutant. Even though these are very rough calculations, they suggest that a large fraction of the proton motive force is used for various transport processes rather than for ATP synthesis.

Table 7
Comparison of different parameters of ΔF_1F_O mutants of *C. glutamicum* (this work), *E. coli* [47,48] and *B. subtilis* [49]. The values for the different parameters are given in % of the corresponding wild type values. n.d., not determined.

Parameter	*C. glutamicum*	*E. coli*	*B. subtilis*
Growth rate	47% (0.19 vs. 0.40 h^{-1})	79% (0.41 vs. 0.53 h^{-1})	66% (0.49 vs. 0.74 h^{-1})
Growth yield	65% (46 vs. 71 g CDW/mol glucose)	58% (46 vs. 80 g CDW/mol glucose)	56% (47 vs. 83 g CDW/mol glucose)
Respiration rate	Increased	139% (17.2 vs. 12.4 mmol O_2/h/g CDW)	182% (73 vs. 48 nmol O_2/min/OD unit)
Membrane potential	115% at pH 7.0 (−220 vs. −192 mV) 131% at pH 6.0 (−172 vs. −131 mV)	120% (−184 vs. −154 mV)	n.d.
[ATP]/[ADP] ratio	n.d.	37% (7 vs. 19)	53% (8 vs. 15)
Cytochromes of *b*-type	Increased	180%	n.d.
Cytochromes of *d*-type	Increased	n.d.	n.d.

Acknowledgments

Financial support (grant 0315598 to MB and KM) by the Bundesministerium für Bildung und Forschung (BMBF) is gratefully acknowledged. The authors would like to thank Dr. Melanie Brocker for the help with MALDI-TOF-MS measurements, Brita Weil and Ulrike Viets for excellent technical assistance, and Prof. Reinhard Krämer (Universität zu Köln) for his support of the measurements of bioenergetic parameters.

Appendix A. Supplementary data

Supplementary data to this article can be found online at doi:10.1016/j.bbabio.2011.10.006.

References

[1] L. Eggeling, M. Bott, Handbook of *Corynebacterium glutamicum*, Taylor & Francis, Boca Raton, 2005.
[2] A. Burkovski, Corynebacteria: genomics and molecular biology, Caister Academic Press, Norfolk, U.K., 2008
[3] M. Bott, A. Niebisch, The respiratory chain of *Corynebacterium glutamicum*, J. Biotechnol. 104 (2003) 129–153.
[4] A. Niebisch, M. Bott, Purification of a cytochrome bc_1-aa_3 supercomplex with quinol oxidase activity from *Corynebacterium glutamicum* — identification of a fourth subunit of cytochrome aa_3 oxidase and mutational analysis of diheme cytochrome c_1, J. Biol. Chem. 278 (2003) 4339–4346.
[5] A. Kabus, A. Niebisch, M. Bott, Role of cytochrome *bd* oxidase from *Corynebacterium glutamicum* in growth and lysine production, Appl. Environ. Microbiol. 73 (2007) 861–868.

[6] Y. Kabashima, J. Kishikawa, T. Kurokawa, J. Sakamoto, Correlation between proton translocation and growth: genetic analysis of the respiratory chain of *Corynebacterium glutamicum*, J. Biochem. 146 (2009) 845–855.
[7] H. Sekine, T. Shimada, C. Hayashi, A. Ishiguro, F. Tomita, A. Yokota, H^+-ATPase defect in *Corynebacterium glutamicum* abolishes glutamic acid production with enhancement of glucose consumption rate, Appl. Microbiol. Biotechnol. 57 (2001) 534–540.
[8] R. Aoki, M. Wada, N. Takesue, K. Tanaka, A. Yokota, Enhanced glutamic acid production by a H^+-ATPase-defective mutant of *Corynebacterium glutamicum*, Biosci. Biotechnol. Biochem. 69 (2005) 1466–1472.
[9] L. Li, M. Wada, A. Yokota, A comparative proteomic approach to understand the adaptations of an H^+-ATPase-defective mutant of *Corynebacterium glutamicum* ATCC14067 to energy deficiencies, Proteomics 7 (2007) 3348–3357.
[10] M. Barriuso-Iglesias, C. Barreiro, F. Flechoso, J.F. Martin, Transcriptional analysis of the F_0F_1 ATPase operon of *Corynebacterium glutamicum* ATCC 13032 reveals strong induction by alkaline pH, Microbiology 152 (2006) 11–21.
[11] C. Keilhauer, L. Eggeling, H. Sahm, Isoleucine synthesis in *Corynebacterium glutamicum*: molecular analysis of the *ilvB-ilvN-ilvC* operon, J. Bacteriol. 175 (1993) 5595–5603.
[12] A. Niebisch, M. Bott, Molecular analysis of the cytochrome bc_1-aa_3 branch of the *Corynebacterium glutamicum* respiratory chain containing an unusual diheme cytochrome c_1, Arch. Microbiol. 175 (2001) 282–294.
[13] A. Schäfer, A. Tauch, W. Jäger, J. Kalinowski, G. Thierbach, A. Pühler, Small mobilizable multi-purpose cloning vectors derived from the *Escherichia coli* plasmids pK18 and pK19: selection of defined deletions in the chromosome of *Corynebacterium glutamicum*, Gene 145 (1994) 69–73.
[14] M.E. van der Rest, C. Lange, D. Molenaar, A heat shock following electroporation induces highly efficient transformation of *Corynebacterium glutamicum* with xenogeneic plasmid DNA, Appl. Microbiol. Biotechnol. 52 (1999) 541–545.
[15] H.U. Bergmeyer, E. Berndt, F. Schmidt, H. Storck, Glucose test, in: H.U. Bergmeyer, K. Gawehn (Eds.), Methods of Enzymatic Analysis, Verlag Chemie, Weinheim, 1974, pp. 1241–1246.
[16] C. Wittmann, H.M. Kim, G. John, E. Heinzle, Characterization and application of an optical sensor for quantification of dissolved O_2 in shake-flasks, Biotechnol. Lett. 25 (2003) 377–380.
[17] G.M. Seibold, S. Dempf, J. Schreiner, B.J. Eikmanns, Glycogen formation in *Corynebacterium glutamicum* and role of ADP-glucose pyrophosphorylase, Microbiology 153 (2007) 1275–1285.
[18] G.M. Seibold, B.J. Eikmanns, The *glgX* gene product of *Corynebacterium glutamicum* is required for glycogen degradation and for fast adaptation to hyperosmotic stress, Microbiology 153 (2007) 2212–2220.
[19] H.M. Woo, S. Noack, G.M. Seibold, S. Willbold, B.J. Eikmanns, M. Bott, Link between phosphate starvation and glycogen metabolism in *Corynebacterium glutamicum*, revealed by metabolomics, Appl. Environ. Microbiol. 76 (2010) 6910–6919.
[20] E. Castiglioni, E. Grilli, S. Sanguinett, A new simple and low cost scattered transmission accessory for commercial double beam ultra-visible spectrophotometers, Rev. Sci. Instrum. 68 (1997) 4288–4289.
[21] M. Follmann, I. Ochrombel, R. Krämer, C. Trötschel, A. Poetsch, C. Rückert, A. Hüser, M. Persicke, D. Seiferling, J. Kalinowski, K. Marin, Functional genomics of pH homeostasis in *Corynebacterium glutamicum* revealed novel links between pH response, oxidative stress, iron homeostasis and methionine synthesis, BMC Genomics 10 (2009) 621.
[22] E.R. Kashket, The proton motive force in bacteria: a critical assessment of methods, Annu. Rev. Microbiol. 39 (1985) 219–242.
[23] H. Rottenberg, The measurement of membrane potential and DpH in cells, organelles, and vesicles, Methods Enzymol. 55 (1979) 547–569.
[24] V.F. Wendisch, Genome-wide expression analysis in *Corynebacterium glutamicum* using DNA microarrays, J. Biotechnol. 104 (2003) 273–285.
[25] N. Möker, M. Brocker, S. Schaffer, R. Krämer, S. Morbach, M. Bott, Deletion of the genes encoding the MtrA-MtrB two-component system of *Corynebacterium glutamicum* has a strong influence on cell morphology, antibiotics susceptibility and expression of genes involved in osmoprotection, Mol. Microbiol. 54 (2004) 420–438.
[26] J. Kalinowski, B. Bathe, D. Bartels, N. Bischoff, M. Bott, A. Burkovski, N. Dusch, L. Eggeling, B.J. Eikmanns, L. Gaigalat, A. Goesmann, M. Hartmann, K. Huthmacher, R. Krämer, B. Linke, A.C. McHardy, F. Meyer, B. Möckel, W. Pfefferle, A. Pühler, D.A. Rey, C. Rückert, O. Rupp, H. Sahm, V.F. Wendisch, I. Wiegrabe, A. Tauch, The complete *Corynebacterium glutamicum* ATCC 13032 genome sequence and its impact on the production of L-aspartate-derived amino acids and vitamins, J. Biotechnol. 104 (2003) 5–25.
[27] J. Frunzke, V. Engels, S. Hasenbein, C. Gätgens, M. Bott, Co-ordinated regulation of gluconate catabolism and glucose uptake in *Corynebacterium glutamicum* by two functionally equivalent transcriptional regulators, GntR1 and GntR2, Mol. Microbiol. 67 (2008) 305–322.
[28] S. Schaffer, B. Weil, V.D. Nguyen, G. Dongmann, K. Günther, M. Nickolaus, T. Hermann, M. Bott, A high-resolution reference map for cytoplasmic and membrane-associated proteins of *Corynebacterium glutamicum*, Electrophoresis 22 (2001) 4404–4422.
[29] D.J.C. Pappin, P. Hojrup, A.J. Bleasby, Rapid identification of proteins by peptide-mass fingerprinting, Curr. Biol. 3 (1993) 327–332.
[30] D.J. Reinscheid, S. Schnicke, D. Rittmann, U. Zahnow, H. Sahm, B.J. Eikmanns, Cloning, sequence analysis, expression and inactivation of the *Corynebacterium glutamicum pta-ack* operon encoding phosphotransacetylase and acetate kinase, Microbiology 145 (1999) 503–513.
[31] M. Bott, Offering surprises: TCA cycle regulation in *Corynebacterium glutamicum*, Trends Microbiol. 15 (2007) 417–425.
[32] W.W. Choi, S.D. Park, S.M. Lee, H.B. Kim, Y. Kim, H.S. Lee, The *whcA* gene plays a negative role in oxidative stress response of *Corynebacterium glutamicum*, FEMS Microbiol. Lett. 290 (2009) 32–38.
[33] J.-S. Park, S. Shin, E.-S. Kim, P. Kim, Y. Kim, H.-S. Lee, Identification of SpiA that interacts with *Corynebacterium glutamicum* WhcA using a two-hybrid system, FEMS Microbiol. Lett. 322 (2011) 8–14.
[34] T.H. Kim, J.S. Park, H.J. Kim, Y. Kim, P. Kim, H.S. Lee, The *whcE* gene of *Corynebacterium glutamicum* is important for survival following heat and oxidative stress, Biochem. Biophys. Res. Commun. 337 (2005) 757–764.
[35] S.D. Park, J.W. Youn, Y.J. Kim, S.M. Lee, Y. Kim, H.S. Lee, *Corynebacterium glutamicum* σ^E is involved in responses to cell surface stresses and its activity is controlled by the anti-sigma factor CseE, Microbiology 154 (2008) 915–923.
[36] Y. Zhu, M.A. Eiteman, R. Altman, E. Altman, High glycolytic flux improves pyruvate production by a metabolically engineered *Escherichia coli* strain, Appl. Environ. Microbiol. 74 (2008) 6649–6655.
[37] S. Sugimoto, I. Shiio, Fructose metabolism and regulation of 1-phosphofructokinase and 6-phosphofructokinase in *Brevibacterium flavum*, Agric. Biol. Chem. 53 (1989) 1261–1268.
[38] A. Yokota, N.D. Lindley, Central metabolism: sugar uptake and conversion, in: L. Eggeling, M. Bott (Eds.), Handbook of *Corynebacterium glutamicum*, Taylor & Francis, Boca Raton, 2005, pp. 399–418.
[39] M.S. Jetten, M.E. Gubler, S.H. Lee, A.J. Sinskey, Structural and functional analysis of pyruvate kinase from *Corynebacterium glutamicum*, Appl. Environ. Microbiol. 60 (1994) 2501–2507.
[40] H. Ozaki, I. Shiio, Regulation of the TCA and glyoxylate cycles in *Brevibacterium flavum*. II. Regulation of phosphoenolpyruvate carboxylase and pyruvate kinase, J. Biochem. 66 (1969) 297–311.
[41] M.E. Schreiner, B.J. Eikmanns, Pyruvate:quinone oxidoreductase from *Corynebacterium glutamicum*: purification and biochemical characterization, J. Bacteriol. 187 (2005) 862–871.
[42] M. Inui, S. Murakami, S. Okino, H. Kawaguchi, A.A. Vertes, H. Yukawa, Metabolic analysis of *Corynebacterium glutamicum* during lactate and succinate productions under oxygen deprivation conditions, J. Mol. Microbiol. Biotechnol. 7 (2004) 182–196.
[43] I. Brune, H. Werner, A.T. Hüser, J. Kalinowski, A. Pühler, A. Tauch, The DtxR protein acting as dual transcriptional regulator directs a global regulatory network involved in iron metabolism of *Corynebacterium glutamicum*, BMC Genomics 7 (2006) 21.
[44] J. Wennerhold, M. Bott, The DtxR regulon of *Corynebacterium glutamicum*, J. Bacteriol. 188 (2006) 2907–2918.
[45] J.A. Imlay, Cellular defenses against superoxide and hydrogen peroxide, Annu. Rev. Biochem. 77 (2008) 755–776.
[46] S. Drose, U. Brandt, The mechanism of mitochondrial superoxide production by the cytochrome bc_1 complex, J. Biol. Chem. 283 (2008) 21649–21654.
[47] P.R. Jensen, O. Michelsen, Carbon and energy metabolism of *atp* mutants of *Escherichia coli*, J. Bacteriol. 174 (1992) 7635–7641.
[48] P.R. Jensen, O. Michelsen, H.V. Westerhoff, Experimental determination of control by the H^+-ATPase in *Escherichia coli*, J. Bioenerg. Biomembr. 27 (1995) 543–554.
[49] M. Santana, M.S. Ionescu, A. Vertes, R. Longin, F. Kunst, A. Danchin, P. Glaser, *Bacillus subtilis* F_0F_1 ATPase: DNA sequence of the *atp* operon and characterization of *atp* mutants, J. Bacteriol. 176 (1994) 6802–6811.
[50] A. Koul, N. Dendouga, K. Vergauwen, B. Molenberghs, L. Vranckx, R. Willebrords, Z. Ristic, H. Lill, I. Dorange, J. Guillemont, D. Bald, K. Andries, Diarylquinolines target subunit c of mycobacterial ATP synthase, Nat. Chem. Biol. 3 (2007) 323–324.
[51] A. Koul, L. Vranckx, N. Dendouga, W. Balemans, I. Van den Wyngaert, K. Vergauwen, H.W. Gohlmann, R. Willebrords, A. Poncelet, J. Guillemont, D. Bald, K. Andries, Diarylquinolines are bactericidal for dormant mycobacteria as a result of disturbed ATP homeostasis, J. Biol. Chem. 283 (2008) 25273–25280.
[52] S.L. Tran, G.M. Cook, The F_1F_0-ATP synthase of *Mycobacterium smegmatis* is essential for growth, J. Bacteriol. 187 (2005) 5023–5028.
[53] B.J. Koebmann, H.V. Westerhoff, J.L. Snoep, D. Nilsson, P.R. Jensen, The glycolytic flux in *Escherichia coli* is controlled by the demand for ATP, J. Bacteriol. 184 (2002) 3909–3916.
[54] D.W. Tempest, O.M. Neijssel, The status of Y_{ATP} and maintenance energy as biologically interpretable phenomena, Annu. Rev. Microbiol. 38 (1984) 459–486.
[55] R.K. Thauer, K. Jungermann, K. Decker, Energy conservation in chemotrophic anaerobic bacteria, Bacteriol. Rev. 41 (1977) 100–180.
[56] S. Abe, K. Takayama, S. Kinoshita, Taxonomical studies on glutamic acid producing bacteria, J. Gen. Appl. Microbiol. 13 (1967) 279–301.